

Title	The volume scanner optical performance
Authors	Vafa, Elham;Holdsworth, John;Sharafutdinova, Galiya;Andersson-Engels, Stefan
Publication date	2017
Original Citation	Vafa, E., Holdsworth, J., Sharafutdinova, G. and Andersson-Engels, S. (2017) 'The volume scanner optical performance', SPIE Proceedings Vol. 10412, European Conferences on Biomedical Optics, 25-29 June, 1041207 (3pp). doi: 10.1117/12.2285313
Type of publication	Conference item
Link to publisher's version	https://www.osapublishing.org/abstract.cfm?uri=ECBO-2017-1041207 - 10.1117/12.2285313
Rights	© 2017, SPIE. All rights reserved.
Download date	2023-05-07 22:09:39
Item downloaded from	http://hdl.handle.net/10468/6900

The Volume Scanner Optical Performance

Elham Vafa^{1*}, John Holdsworth¹, Galiya Sharafutdinova¹, Stefan Andersson-Engels²

¹School of Mathematical and Physical Sciences, The University of Newcastle, Callaghan 2308 NSW, ²Tyndall National Institute, Lee Maltings Complex, Dyke Parade, Cork, T12R5CP Ireland

*elham.vafa@uon.edu.au

Abstract: The optical performance of a volume scanner is analyzed using modelling software. The existence of an embedded scattering volume with a 2.5% difference in scattering coefficient from the host media may be detected.

OCIS codes: (170.0170) Medical optics and biotechnology; (080.0080) Geometric optics

1. Introduction

Breast cancer is the main contributor to cancer related deaths among women worldwide, with nearly 13 million breast cancer deaths expected globally over the next 25 year period [1]. This is a powerful driver for us and others toward developing a sophisticated optical diagnostic cancer screening system where imaging of a pendant breast is achieved by illuminating with a harmless optical light source, and recording the light transmitted and scattered through the breast tissue followed by a tomographic reconstruction process to create a 3D breast image. As light travels through breast tissue, it is effectively diffused by the macroscopic structures within the tissue including; blood vessels; fatty tissue; lymph nodes; lactation ducts; supporting muscles and fibrous tissues; skin; as well as the intracellular components [2,3]. Thus, the tissue optical properties are characterized by the collective absorption and scattering parameters of the tissue as a whole and the optical investigation of the breast is achieved by measuring the light intensity diffusing from the light source locations to a set of detector locations [4,5]. The optical characterization of the breast may be achieved by calculating the photon path length inside the breast [6]. The greater number of blood vessels and the reduced lipid content of tumors [3] may be used to distinguish between cancerous and healthy tissue. As a result, from a physics point of view, breast lesions can be seen as localized absorption and scattering perturbations embedded in homogeneous diffusive tissue. It is the relative increase in scattering characteristics for those zones that can be used for cancer detection [6].

In most optical breast cancer studies, near-infrared light in the spectral window between the hemoglobin and water absorption bands (650nm - 1100nm) [3,7] has been used to illuminate the breast due to the larger penetration of this wavelength band inside soft, scattering tissue as the tissue is rather transparent up to several centimeters in depth [8].

This paper presents the optical performance evaluation of our proposed 3D scanner as detailed in [9]. The volume scanner uses dual parabolic reflectors with the potential to be a future optical mammography system for pendant breasts. The detection is anticipated to be a time-gated, intensified Megapixel array with photon counting capability. The proposed volume scanner is simulated via TracePro optical design software to investigate its optical performance and validate the design functionality. The reconstruction algorithm used to reconstruct an image is out of scope of this paper.

2. Scanner optical design via computer simulation

The TracePro software (Lambda Research Corporation) uses a Monte Carlo based ray tracing engine to simulate the distribution of rays propagating through the volume scanner [9]. A light source is modelled as a number of rays distributed uniformly in rings, with each ray individually traced through the scanner and the result evaluated by a number of rays striking an image surface to generate an irradiance map. The optical scanner design is shown in Fig. 1 [9,10].

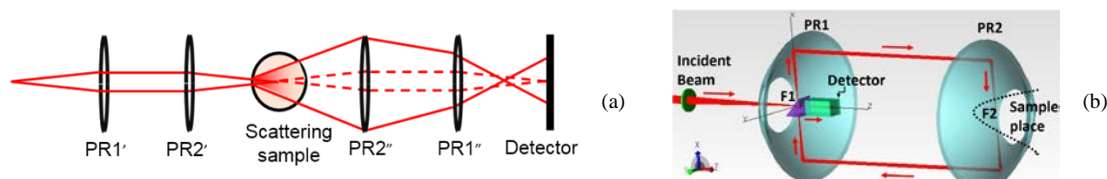


Fig. 1. (a) Effective equivalent optical train of the volume scanner and, (b) schematic TracePro design

The prototype scanner has been constructed with dual 150 mm diameter, 30 mm focal length parabolic reflectors with a rear aperture of 35 mm Edmund Optics, PR1 and PR2 that are separated by 580 mm on the z-axis as shown schematically in Fig. 1(b). The sample to be investigated is positioned inside the PR2 volume. An incident He-Ne laser

beam (632.8 nm, 2 mW), is modelled as a circular grid array with Gaussian intensity profile, and is focused by a 150 mm f.l. lens (Thorlabs) to a spot on the right prism hypotenuse co-located with the focal point of the parabolic reflector PR1. When there is no sample present, a collimated beam travels to PR2, reflects at 90 degrees, passes through its focus and is re-collimated by reflection, returning as a parallel beam to PR1, where it is again focused and totally internally reflected at the prism hypotenuse. The reflected beam expands and is incident upon a detector surface modelled as a 50×50 grid. The received total number of rays is recorded as an illumination map on the 225 mm^2 flat square detector surface. When a sample is present inside the PR2 volume, the passage of the light on the illumination side is unaffected. On the detection side, however, a large numerical aperture of scattered light from the sample is collected by PR2 and relayed to the detector. The distance between PR1 and PR2 can be varied along the z-axis (Fig. 1(b)) and the prism can be rotated 360 degrees to provide the volume scan. Fruit samples and gelatin based phantoms have been predominantly used as samples in the modeling, as their optical properties match the physical features of biological media [11]. The scattering sample investigated in this paper is modelled as a 4 mm diameter spherical volume embedded off-axis inside a gelatin-filled, cylindrical glass vial (44.4 mm long, 9.5 mm outer radius and 1 mm wall thickness). To reduce the unwanted scattered light, shrouds are used to cover the glass vial. For this investigation, the distance between the parabolic reflectors is fixed.

3. Results and Discussion

3.1. Optical performance of the scanner without sample

To investigate the optical performance of the scanner itself, three different laser beam radii were used to propagate through the scanner without a sample. The detected logarithmic contour plots for the light source array of $\sim 100,000$ rays, distributed uniformly in 183 rings are shown in Fig. 2. The beam footprints on the detector indicate the excellent optical performance of the scanner as all the injected rays form distortion-free uniform patterns at the detector surface.

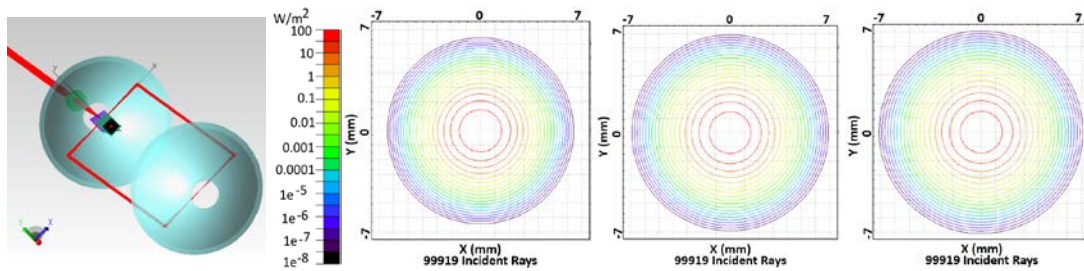


Fig. 2. Volume scanner (a) and logarithmic beam contour plots for beam radius of; (b) 1 mm; (c) 4 mm; (d) 15 mm.

3.2. Scattering sample

A scattering sample of a cylindrical glass vial filled with gelatin ($\mu_s = 0.15 \text{ mm}^{-1}$) is positioned on-axis as shown in Fig. 3(a) and illuminated by 4 mm radius laser beam modelled with 99919 rays. Fig. 3(b) shows the scanner performance without a sample including the detected illumination map with all rays reaching the detector. Fig. 3(c) shows a reduced set of 14158 rays reaching the detector following beam scatter through the sample and the refraction induced by the cylindrical symmetry of the vial and sample.

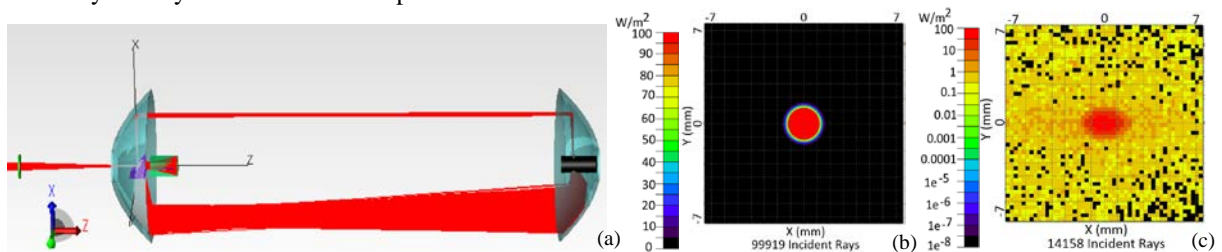


Fig. 3. Volume scanner (a) with cylindrical sample. Detected rays, (b) without sample, (c) with sample

3.3. Scattering sample with embedded scattering element

In order to examine whether differences in scatter could be determined by the system, a spherical scattering sample was embedded within the gelatin filled cylindrical vial (Fig. 4(a)). The scattering coefficient for the inserted volume was varied incrementally over the range; 0.9; 1.01; 1.025; 1.05; 1.1; 1.2; 1.4; 1.6; 1.8 and; 2 times the gelatin scattering coefficient ($\mu_s=0.15 \text{ mm}^{-1}$) with the detected number of rays decreasing as shown in Fig. 4(b). This result is a clear demonstration of the scanner performance. These data represent three trials based on different random seed numbers for Monte Carlo calculations for each set of ray traces. Outcomes of this modelling experiment obviously demonstrate the scanner's ability to detect differences in samples and it is possible to discern a measurable difference in the integrated scatter recorded with a 2.5% change in the scattering coefficient of the embedded volume.

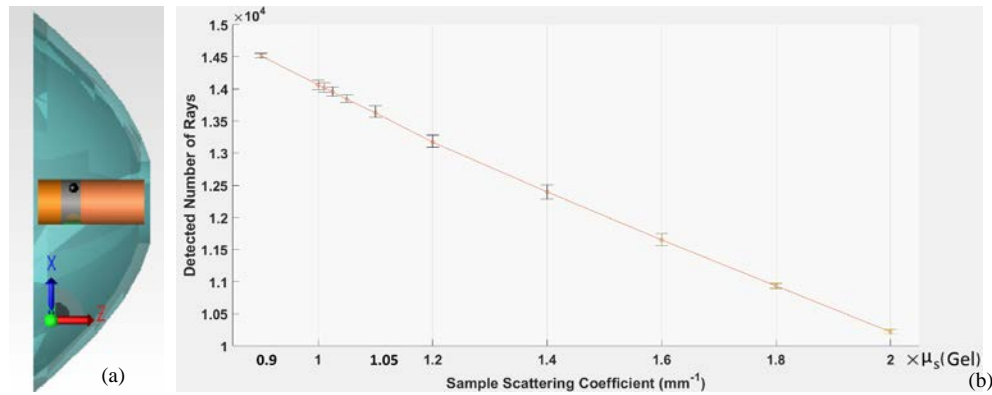


Fig. 4. (a) Spherical sample inside cylindrical vial, (b) Number of rays reaching the detector for small variation of an embedded μ_s .

4. Conclusion

The proposed volume scanner demonstrates excellent optical performance and is able to distinguish the existence of an embedded scattering medium in the system when there is a difference of 2.5% in the scattering coefficient for a volume inserted in different diffuse media. The tomographic reconstruction algorithms for the system are under study.

4. References

- [1] S. G Komen, "Breast Cancer Statistics", <http://ww5.komen.org/BreastCancer/Statistics.html> (2017).
- [2] Colak,S., Van der Mark,M., Hooft, G. t, Hoogenraad,J., Van der Linden,E. and Kuijpers,F., "Clinical optical tomography and NIR spectroscopy for breast cancer detection," IEEE Journal of selected topics in quantum electronics, Vol. 5, no. 4, IEEE Photonics Society, 1143-1158 (1999).
- [3] Taroni,P., "Diffuse optical imaging and spectroscopy of the breast: a brief outline of history and perspectives," Photochemical & Photobiological Sciences, vol. 11, no. 2, 241-250 (2012).
- [4] Dehghani,H., Pogue,B. W., Poplack,S. P. and Paulsen, K. D., "Multi wavelength three dimensional near-infrared tomography of the breast: initial simulation, phantom, and clinical results," Applied Optics, vol. 42, no. 1, 135-145 (2003).
- [5] Enfield, L. C., Gibson, A. P., Everdell, N. L., Delpy, D. T., Schweiger,M., Arridge, S. R., Richardson, C., Keshtgar,M., Douek, M. and Hebden, J. C., "Three-dimensional time-resolved optical mammography of the uncompressed breast," Applied optics, vol. 46, no. 17, 3628-3638 (2007).
- [6] Quarto,G., Pieri,A., Cubeddu,R., Ieva,F., Paganoni, A. M., Abbate,F., Cassano, E. and Taroni,P., "Optical discrimination between malignant and benign breast lesions?" in European Conferences on Biomedical Optics, International Society for Optics and Photonics, 953814-953814 (2015).
- [7] Grosenick,D., Moesta,K. T., Wabnitz, H., Mucke, J., Stroszczynski, C., Macdonald, R., Schlag, P. M. and Rinneberg,H., "Time-domain optical mammography: initial clinical results on detection and characterization of breast tumors," Applied optics, vol. 42, no. 16, 3170-3186 (2003).
- [8] Menke,J., "Photoacoustic breast tomography prototypes with reported human applications," European Society of Radiology, vol. 25, no. 8, (2015).
- [9] Vafa, E., Roberts, N., Sharafutdinova, G. and Holdsworth, J., "A volume scanner for diffuse imaging," Proc. SPIE 10013, SPIE BioPhotonics Australasia, doi:10.1117/12.2242971 (2016).
- [10] Sharafutdinova,G., Holdsworth,J., Hosseini,A., Vafa,E. and Van Helden,D., "Investigating a new volume scanner," in Australian and New Zealand Optics and Photonics,1-3 (2013).
- [11] Askoura, M. L., Piron, V., Vaudelle, F., L'Huillier, J.-P., Madieta, E., and Mehinagic, E., "Experimental investigation on light propagation through apple tissue structures." SPIE 9542, 954218-954218-954219 (2015).